



OPEN

Qualifying interfacial properties of crude oil–water system with the synergistic action of a nano Gemini ionic liquid and conventional surfactants

Javad Saïen , Asma Eghtenaei & Mona Kharazi 

Surface-active ionic liquids (SAILs) have gained much attention due to their green, stable, and efficient properties. The high costs associated with SAILs have raised concerns in their applications; however, blending with conventional surfactants like sodium dodecyl benzene sulfonate (SDBS) can bring about desired outcomes. Gemini surface-active ionic liquids (GSAILs) have been recognized as more efficient surfactants. Accordingly, this study investigates the influence of a mixture of an imidazolium-based GSAIL, $[C_4im-C_6-imC_4][Br_2]$, and SDBS on different aspects of crude oil–water interfacial properties. The findings show remarkable synergy in interfacial tension (IFT) reduction up to 98.8% together with incredibly low IFT value of 0.05 mN m^{-1} . This was with an optimal GSAIL mole fraction of 0.2 in the mixture. Further, the surfactant mixture gives synergies of 52.6% in emulsification and 51.8% in wettability of a quartz surface. These amazing results can be explained by the dominant interactions between the oppositely charged components. In theoretical study, the adsorption of individual surfactants and their mixtures was analyzed based on the Frumkin isotherm and the Rosen model, respectively, further supporting the findings.

Keywords Ionic liquids, Interfacial tension, SDBS, Wettability, Emulsification

The world demand on crude oil is steadily increasing whereas primary and secondary recovery methods could only extract 20 to 40% of reservoir crude oils¹. Thus a growing interest has been developed on alternative enhanced oil recovery (EOR) techniques with a significant focus on surfactant application^{2,3}. Use of traditional surfactants usually face limitations in EOR because of sensitivity to operating conditions such as salinity and temperature⁴. In contrast, amphiphilic surface-active ionic liquids (SAILs) are considered as promising materials due to their favorable activity and environmental advances such as stability, low toxicity, recyclability and low vapor pressure^{5,6}.

From an economic standpoint, SAILs are considerably expensive⁷, and that for valuable EORs, the crude oil–water interfacial tension (IFT) needs to be at very low values; hence, use of a SAIL could not be economy⁴. However, blending with conventional surfactants can develop a synergy with extensive IFT reduction. Accordingly, it has been represented that blends of opposite charged surfactants can significantly influence the IFT of (toluene + n-decane)–water system⁸. Additionally, it has been demonstrated that different mixtures of a single-chain SAIL with a conventional surfactant can remarkably improve the interfacial properties of the crude oil–water system, making oil recoveries more attainable⁹.

As a subset of SAILs, Gemini surface-active ionic liquids (GSAILs), consisting of two hydrophilic head groups and hydrophobic chain groups linked by a hydrocarbon spacer have received high attention. Desired properties and environmentally friendly characters are emphasized for GSAILs whilst exhibiting high interfacial activity and being resistive against thermal and salinity effects^{10,11}. Of note, among various types of GSAILs (imidazolium, pyrrolidinium, morpholinium and pyridinium), imidazolium ones are with great activity¹². Adding to these, the associated nano-size particles give rise their activities¹³.

Department of Applied Chemistry, Faculty of Chemistry and Petroleum Sciences, Bu–Ali Sina University, Hamedan 6517838695, Iran. ✉email: saïen@basu.ac.ir; jsaïen@yahoo.com

In this context, the medium-chain-length GSAIL $[C_8im-C_4-C_8im][Br]_2$ was synthesized in nano-size for the first time by Saïen et al.¹⁴. The investigation focuses on the interfacial properties of the used GSAIL at different temperatures and salty solutions. The results demonstrated its great performance in reducing IFT and forming stable oil–water emulsions, even under elevated temperatures and salt concentrated conditions. In, another study by Ding et al.¹⁵, demulsification performance of a GSAIL was investigated. The results indicated that the GSAIL achieved 100% efficiency compared to conventional surfactants. Additionally, Wang et al.¹⁶ studied the interfacial properties of a mixture of the cationic Gemini ammonium surfactant (16–4–16) and SDBS. Their findings revealed a strong synergistic effect between the surfactants, leading to significant reductions in IFT and critical micelle concentration (CMC).

In the continuity of our studies on different aspects of EOR^{17–19}, this study was dedicated to examine how the presence of imidazolium cationic GSAIL, namely $[C_4im-C_6-imC_4][Br]_2$ (structured with two C_4 alkyl chains linked with a C_6 alkyl chain spacer) mixed with the anionic surfactant of sodium dodecyl benzene sulfonate (SDBS) works in EOR. Considering the fact that most EOR studies are concerned on using single-chain SAILs, utilizing mixtures of powerful imidazolium-based GSAILs and SDBS for different aspects of EOR are potentially beneficial. The extent of IFT reduction and corresponding CMC as well as capability in emulsion formation and wettability alteration are investigated for the crude oil–water system. These are important parameters determining pore-scale oil/water distributions and thus with serious effects in reservoir-scale oil production.

Accordingly, the impact of individual surfactants are first considered. Next, the level of synergism in reducing IFT and CMC using surfactant mixtures are investigated. The results are then analyzed based on the Frumkin isotherm and the Rosen non-ideal interactions in binary mixtures (NIBM) model. Finally, this study assesses the impact of these mixtures on emulsion formation and wettability alteration.

Experimental Materials

The examined crude oil was from the Ahwaz oil field in south Iran for which the major specifications are tabulated in Table 1. The 99% pure SDBS surfactant was a Sigma Aldrich product. The synthesized imidazolium cationic GSAIL was comprised of four carbon atoms alkyl chains and six methylene in the spacer as well as two bromine anions, totally denoted as [1, 1'-(hexane-1, 6-diyl) bis (3-butyl-1*H*-imidazol-3-ium) bromide], concisely abbreviated as $[C_4im-C_6-C_4im][Br]_2$ (Fig. 1). This GSAIL was prepared according to a reported procedure²⁰. To ensure GSAIL quality and nano-size product, ¹H NMR, ¹³C NMR, dynamic light scattering (DLS) and scanning

| Spicification/Composition | Value |
|--|-------|
| °API | 20.7 |
| Saturated (wt%) | 54.0 |
| Aromatic (wt%) | 22.3 |
| Resin (wt%) | 6.7 |
| Asphalt (wt%) | 7.7 |
| Acidity number (mg KOH g ⁻¹) | 0.09 |
| Sulphur content (wt%) | 1.63 |
| Salt content (lbs per 1000 bbls) | 4 |
| Water content (wt%) | Nil |
| Density at 20 °C (g cm ⁻³) | 0.915 |
| Viscosity at 70 °F (cP) | 55 |
| Viscosity at 100 °F (cP) | 44 |
| Kinematic viscosity at 70 °F (cSt) | 60 |
| Pour point (°F) | 10 |
| Flashpoint (°F) | 70 |
| Reid vapor pressure (psi) | 12.1 |
| Loss at 200 °C (wt%) | 9.3 |

Table 1. Most important crude oil specifications.

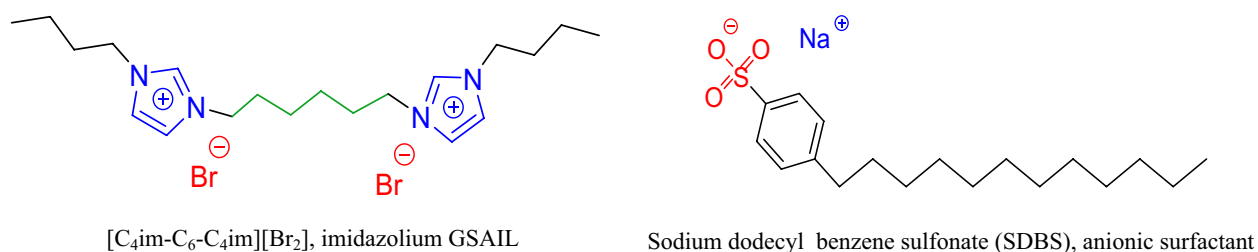


Fig. 1. The used surfactants chemical structures.

electron microscopy (SEM) were employed. Analytical results are provided in Figs. S1 to S4 (Supplementary Material). The high purity of the product was proved by appearing specific peaks of the prepared imidazolium GSAIL as in the NMR spectra with no sign of the reactants or any by-product. The hydrodynamic and micelle size of the as prepared product were examined via SEM and DLS methods as listed in Table 2. It is important to note that the obtained size via DLS, referred as "hydrodynamic size", pertains to the GSAIL particles in aqueous solution which is different from that of particle size observed in SEM. Aqueous phase solutions were prepared using a high quality distilled water. For convenient understanding, the chemical structure of the GSAIL and SDBS surfactants are illustrated in Fig. 1.

Instruments and procedures

IFT and contact angle measurements

The IFT and contact angle (CA) measurements were performed by means of a pendant drop tensiometer (CA-ES10, Fars EOR Technology). For this aim, crude oil was conducted to the tip of a suitably size stainless steel needle, which was submerged in the aqueous bulk solution. The experimental setup and methodology were thoroughly explained in our previous publications^{21,22}. The IFT (γ) was detected at different times by considering the geometric shape of the pendant drop with respect to the involved forces monitored and analyzed by an image processor²³. Through this technique, an equilibrium IFT equal to $31.8 \text{ mN}\cdot\text{m}^{-1}$ was detected for the crude oil – pure water at 298.2 K. Meanwhile, the surface tension of water was determined to be $71.9 \text{ mN}\cdot\text{m}^{-1}$ at the same temperature, remarkably close to the literature reported value of $72.0 \text{ mN}\cdot\text{m}^{-1}$ ²⁴. These measurements were conducted under ambient pressure, and temperature was maintained constant by means of a thermostat (uncertainty of 0.1 K).

The surfactants, individually and in mixtures, were utilized within a concentration range of 1.0×10^{-4} to $1.25 \text{ mol}\cdot\text{dm}^{-3}$, were prepared by mass utilizing a $1.0 \times 10^{-4} \text{ g}$ digital balance. Mixing of components was based on the GSAIL mole fraction, $\alpha_1 = C_1/C_{12}$ in which $C_{12}=C_1+C_2$ whereas C_1 and C_2 represent the molar bulk concentrations of the GSAIL and SDBS and C_{12} for the mixture, all in aqueous phase. Meanwhile, an Anton Paar oscillating densitometer (DMA 4500, Austria) was used to determine the density of solutions which is an essential parameter to determine IFT values. The uncertainty of the densitometer was $1.0 \times 10^{-4} \text{ g}\cdot\text{cm}^{-3}$. To determine a CMC, the corresponding concentration at the intersection of tangent lines to the upper and lower regions of the IFT variations against surfactant concentration was considered.

Emulsion formation

Emulsion formation was performed with equal volumes of the aqueous and oil phases. Here, the aqueous phase concentration of individual surfactants/mixtures was $0.05 \text{ mol}\cdot\text{dm}^{-3}$ having significant impact. Samples were transferred to a scaled glass vial and sonicated in an ultrasound bath (40 kHz, 305 W) for 30 min and then were allowed to rest at 298.2 K over one day and one week. After that, the volume of the formed emulsion (V_e) was measured and the emulsion index (in percentage) was obtained from $V_e/V_t \times 100$ where V_t was the sample total volume²⁵.

Wettability alteration measurement

For wettability alteration, measuring CA was the basis. Accordingly a quartz plate was first maintained in crude oil for 15 to 20 h to simulate aging. Then, injection of crude oil into the aqueous phase, containing in a glass cell, was done via a vertical stainless steel needle to create a drop which was released and attached to the upper quartz plate in a cell filled by the aqueous phase²⁶. After allowing the drop to settle over a minimum one hour time, the image was captured and the CA was reported as an average of the right and left sides of the hemispherical drop. Similar to emulsions, a constant $0.05 \text{ mol}\cdot\text{dm}^{-3}$ concentration, though different mole fraction of mixtures, was considered and examined.

Results and discussion

Interfacial tension reduction with individual surfactants

Figure 2 illustrates the IFT variation versus concentration of individual surfactants. A significant IFT reduction is observed till a CMC. For the imidazolium GSAIL and SDBS, the IFT declines from 31.8 to, respectively, 8.8 and $1.2 \text{ mN}\cdot\text{m}^{-1}$ and the CMCs were appeared at 0.68 and $0.03 \text{ mol}\cdot\text{dm}^{-3}$ (Table 3)²⁷. Comparing the imidazolium GSAIL with the conventional surfactant reveals that the longer alkyl chains of 12 C-atoms of the SDBS gives it an edge over the 4 C-atoms short-chain GSAIL. The maximum IFT reduction of more than 96% with SDBS could be compared to about 72% with the GSAIL. Nevertheless, as Fig. 2 demonstrates that imidazolium GSAIL, despite a short alkyl chain, gives almost good IFT reduction. To attain a typical mid IFT of $15 \text{ mN}\cdot\text{m}^{-1}$, the required GSAIL was only $0.15 \text{ mol}\cdot\text{dm}^{-3}$.

| SEM (nm) | DLS (nm) | |
|-----------|--------------|-------------|
| | Hydrodynamic | Micelle |
| 11.9–27.5 | 0.7–5.0 | 199.8–580.2 |

Table 2. The ranges of pure GSAIL particle size by SEM and hydrodynamic and micelle sizes in aqueous solutions by DLS analysis.

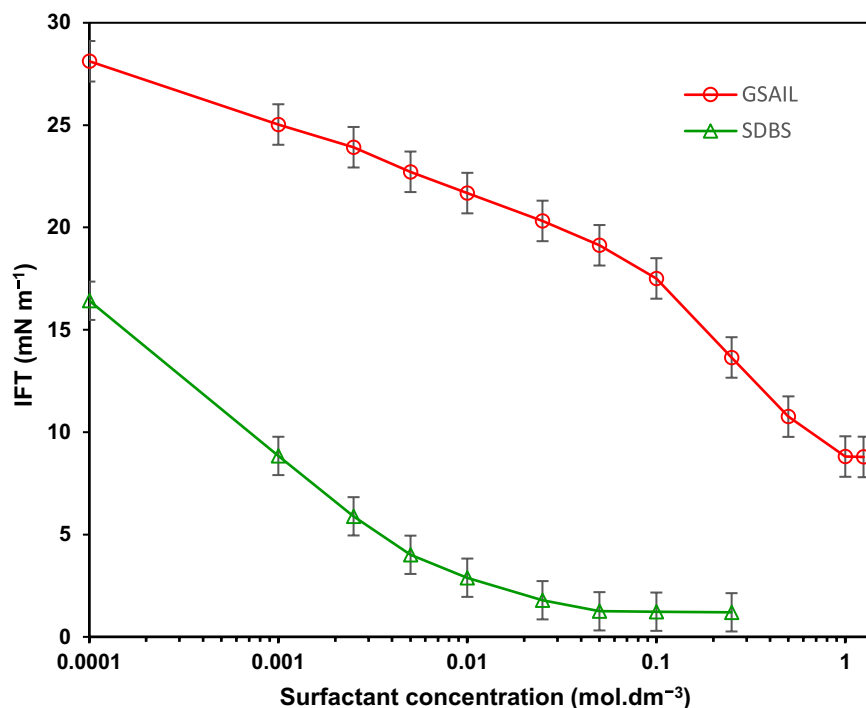


Fig. 2. IFT of the crude oil–water versus concentration of either of surfactants.

| Surfactant | CMC (mol dm ⁻³) | γ_{CMC} (mN m ⁻¹) | γ_{min} (mN m ⁻¹) | Maximum IFT reduction (%) |
|---|-----------------------------|--------------------------------------|--------------------------------------|---------------------------|
| [C ₄ im-C ₆ -imC ₄][Br ₂] | 0.68 | 9.9 | 8.8 | 72.4 |
| SDBS | 0.03 | 1.9 | 1.2 | 96.2 |

Table 3. CMC and IFT under CMC and minimum achieved IFT values for individual surfactants.

The Frumkin adsorption isotherm, which takes into account the non-ideal interactions among adsorbed species, gives a satisfactory explanation for predicting IFT with individual surfactants. With respect to the positive charged rings in the GSAIL structure, and also the negative charge head group in SDBS, one can conclude certain interactions among the surfactant molecules in solutions and in adsorbed layers. The adsorption model and the isotherm of the Frumkin equation are as²⁸:

$$\Pi = -2RT\Gamma_{m,F}[\ln(1 - \theta) + \beta\theta^2] \quad (1)$$

$$b_F f_{\pm} [C(C + C_{\text{electrolyte}})]^{1/2} = \frac{\theta}{1 - \theta} \exp(-n\beta\theta) \quad (2)$$

where $\Pi = \gamma_o - \gamma$ represents the interfacial pressure and γ_o and γ are, respectively, the pure and the present IFT values. Also, $\theta = \Gamma / \Gamma_{m,F}$ represents the fraction of interface coverage, corresponding to Γ and $\Gamma_{m,F}$ (the present and the maximum interface excess concentrations). Parameters b_F , β and f_{\pm} are respectively, the Frumkin adsorption constant, the van der Waals molecular interaction and the activity coefficient of ions. Also, n represents the number of cations and anions of the substance. The accuracy of fittings was based on achieving the lowest value of an objective function (OF) as a fraction of unity, introduced in Ref.²⁹. The parameters obtained from fitting and the corresponding OF values are tabulated in Table 4. Evidently, the Frumkin adsorption isotherm precisely predict the data.

It is obvious that $\Gamma_{m,F}$ of SDBS, possessing long 12 C chain, is greater than that of GSAIL with short 4 C chains. This is in agreement with the previous results relevant to higher hydrophobicity and thus increased interface adsorption. Relatedly, the minimum occupied interface area per adsorbed molecule, A_m , was obtained from $A_m = 1 / \Gamma_{m,F} N_{Av}$ in which N_{Av} represents the Avogadro number. As is expected, SDBS has a more compact orientation at the interface resulting in lower interfacial area per each molecule compared to the GSAIL. Also, the negative molecular interaction parameter, β , confirms intermolecular repulsion. Remarkably, this parameter is greater for the GSAIL which is attributed to the two positively charged rings in the structure. Moreover, the b_F parameter is greater for the conventional surfactant, indicating its superior hydrophobicity and more adsorption

| Surfactant | $\Gamma_{m,F} \times 10^6$ (mol m ⁻²) | $A_m \times 10^{36}$ (m ²) | β | b_F (dm ³ mol ⁻¹) | OF | ΔG_{ads}° (kJ mol ⁻¹) | ΔG_{mic}° (kJ mol ⁻¹) |
|---|---|--|---------|--|-------|--|--|
| [C ₄ im-C ₆ -imC ₄][Br ₂] | 0.77 | 15.13 | -6.2 | 1.53×10^2 | 0.116 | -75.62 | -0.96 |
| SDBS | 0.83 | 13.97 | -2.5 | 6.47×10^4 | 0.391 | -105.58 | -8.69 |

Table 4. The Frumkin and thermodynamic parameters and the objective functions in accordance to the Frumkin isotherm.

tendency. Consistently, the adsorption and micellization Gibbs free energies, are ascertained as following where $\rho' = \rho / 18$ stands for molar concentration of water³⁰:

$$\Delta G_{ads}^\circ = -2RT \ln \left(\frac{b_F \rho'}{2} \right) \quad (3)$$

$$\Delta G_{mic}^\circ = RT \ln \text{CMC} \quad (4)$$

The negative values for the Gibbs free energies listed in Table 4 reinforce understanding that the GSAIL and the SDBS tend to adsorb and form micelle spontaneously. Indeed, the strong hydrophobic nature accompanied with the low electrostatic repulsion, provide a stronger adsorption capability for SDBS. Further, significantly higher absolute values for ΔG_{ads}° implies stronger surfactants tendency to adsorb than forming micelle.

Interfacial tension reduction with surfactants mixtures

Figure 3 illustrates the IFT variation versus mixture concentration when various GSAIL mole fractions (α_1) are attributed. For all the mole fractions, the IFT decreases consistently with concentration. Rationally, the easily adsorption at low concentrations gives more slope of IFT variation (logarithmic scale x-axis) and ultimately with very low IFTs, around 0.05 mN m⁻¹. Notably, low IFTs are coincident with high capillary number in oil reservoirs^{12,31}.

The synergistic action of surfactants could be quantified in comparison to the IFT which could be achieved with the linear contribution of surfactants in each mixture (i.e. no synergism)²⁰. The IFT variations versus α_1 are depicted in Fig. 4. As can be seen, as α_1 increases, the IFT initially decreases sharply and then gradually rises toward the IFT corresponding to the GSAIL ($\alpha_1=1$) under a specified concentration. Regions with a percentage of synergy are marked by distinct colors. The most appropriate 98.8% synergy, relevant to the lowest IFT, was revealed with 0.1 mol dm⁻³ when $\alpha_1=0.2$. In comparison to former investigations on the combination of cationic and anionic surfactants^{9,32}, as well as the mixture of single-chain SAILs and surfactants^{33,34}, the attained here high degree of synergy, proves the strong influence of the GSAIL and SDBS mixtures.

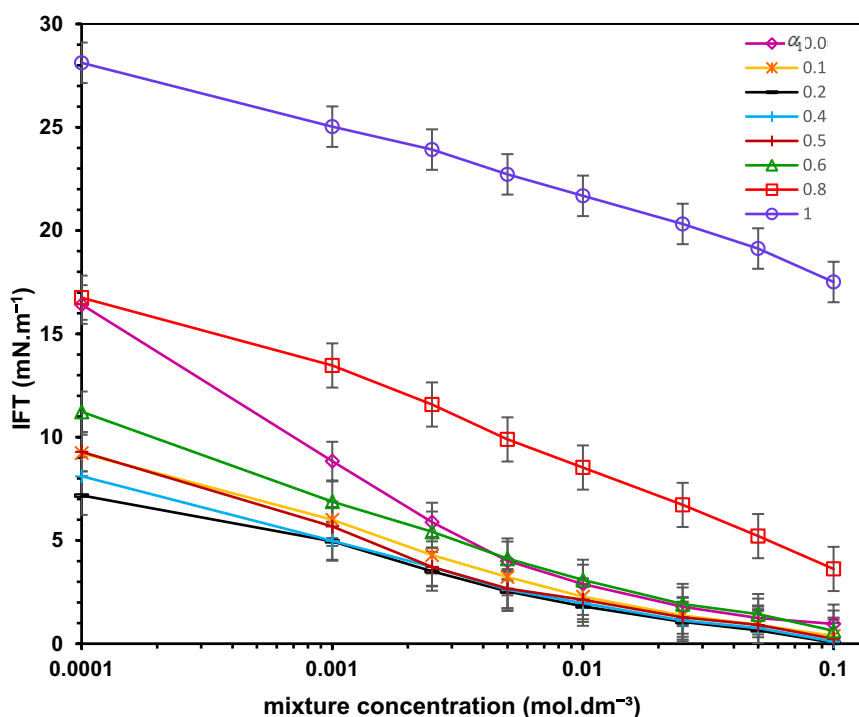


Fig. 3. Variation of the crude oil–water IFT versus mixture concentration for different GSAIL mole fractions.

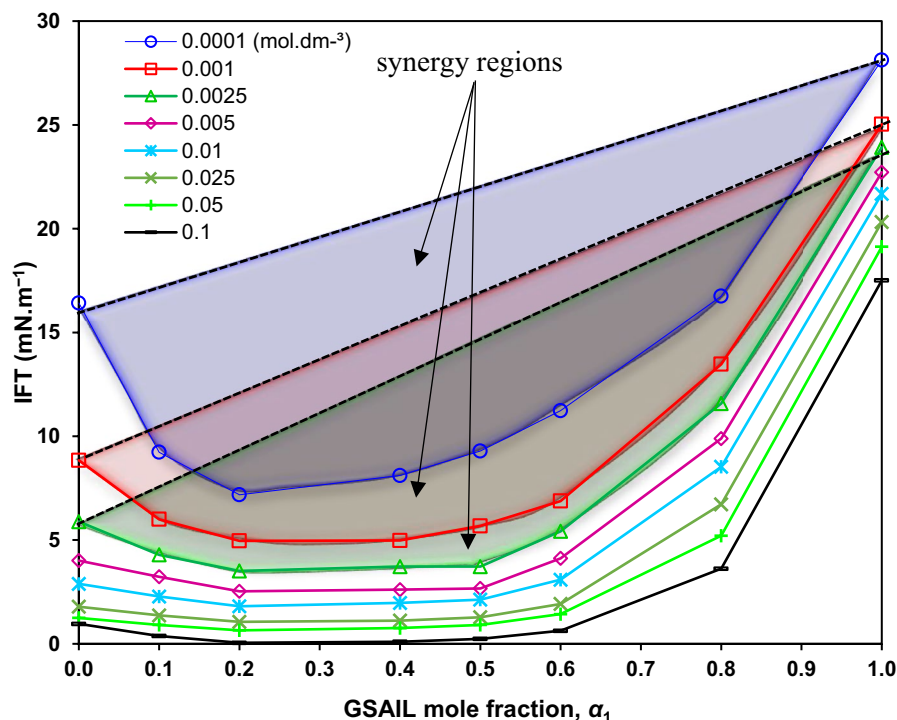


Fig. 4. Synergy regions in IFT reduction for mixtures of the GSAIL and SDBS surfactant.

Examining the surfactants chemical structure (refer to Fig. 1), it is evident that a proximal orientation at the interface is plausible because of the attractive forces between the opposite charge mixture components. Notably, owing to the impact of the single negative charge of SDBS per molecule and the positive charge rings of the GSAIL, it is likely that the maximum synergy to be associated with a GSAIL:SDBS molar ratio of 1:2. However, because of bulkier head groups of the GSAIL, this ratio was revealed with best results when one GSAIL molecule is accompanied with four SDBS molecules, i.e. molar ratio of 1:4 or $\alpha_1 = 0.2$. This finding is quite interesting since an optimal mixture of so much low GSAIL contribution acts so efficient, important also in economic evaluation. As mole fraction increases, the percentage of synergy decreases due to disruptions in the electrostatic balance. Figure 5 depicts the most possible assembly of the considered surfactant molecules and their arrangement at the interface of the crude oil–water system.

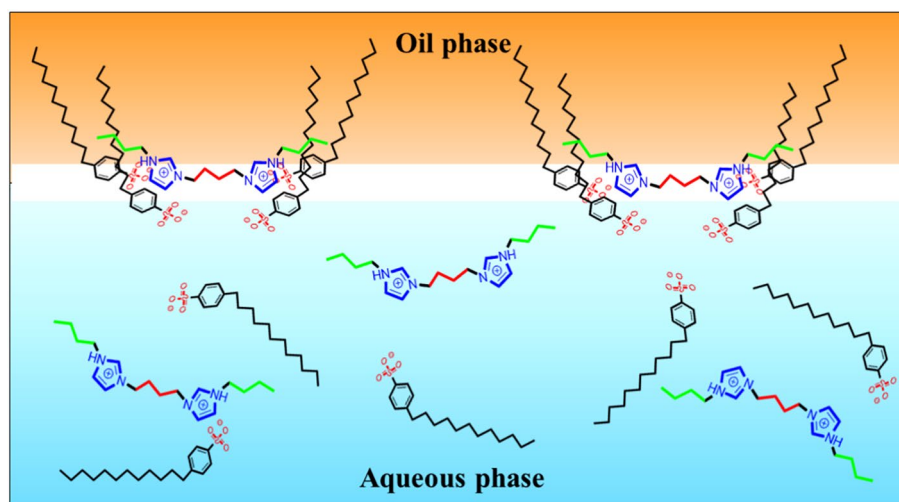


Fig. 5. The assembly of the GSAIL and SDBS molecules and their arrangement at the interface of crude oil–water.

A comparable mechanism could also be attributed to micellization. The CMC, in the present of mixtures, falls to an exceptionally small value of $0.016 \text{ mol dm}^{-3}$ (90.2% synergy compared to presumably linear contribution of surfactants in mixture) at $\alpha_1=0.2$. It is important to emphasize that low CMCs are desirable. This is because low CMCs facilitate the transportation of oil droplets via surfactant flooding in EOR processes⁷. Noteworthy, low CMCs could diminish overall costs because of using minor doses which is highly beneficial in industries.

The NIBM theory⁴ was employed to ascertain the obtained results and determining the adsorbed GSAIL mole fraction (X_1 , designated as surfactant (1) as well as the adsorbed molecular interaction (β), included in the following Eqs. ⁴:

$$\frac{(X_1)^2 \ln(C_{12}\alpha_1 / C_1^0 X_1)}{(1 - X_1)^2 \ln[C_{12}(1 - \alpha_1) / C_2^0(1 - X_1)]} = 1 \quad (5)$$

$$\beta = \frac{\ln(C_{12}\alpha_1 / C_1^0 X_1)}{(1 - X_1)^2} \quad (6)$$

where, C_1^0 , C_2^0 and C_{12}^0 denote the bulk concentration of the GSAIL, of SDBS and of their mixture, all corresponding to a certain IFT. These values are derived from IFT versus surfactant concentration and their mixture for a particular α_1 value (see Fig. 3). Precise X_1 and β values were then calculated from Eqs. (7 and 8) using an iteration method³⁵. Reasonably, negative β values validate an attractive molecular interaction, while positive values indicate repulsive one (in contrary to the Frumkin theory). The corresponding parameter values at certain IFTs are tabulated in Table S1 (Supplementary Material) and Fig. 6a and b show X_1 and β values. It becomes clear that despite self-repulsion between molecules of individual surfactants, an attractive interaction is dominant at the interface. Large absolute β values, in another way, confirm strong synergistic effect³⁶.

Emulsifying ability

Transferring surfactants to low permeable zones in order to facilitating dissolution of crude oils through oil-in-water (O/W) emulsions is important in EOR. This gives rise the crude oil adsorption on reservoir rocks and gives rise residual crude oil flow³⁷. Further, emulsions improve the mobility and sweeping efficiency of injection fluids in non-swept areas^{38,39}. Figure 7 depicts images of emulsions with various mixtures under a typical 0.05 mol dm^{-3} of mixture concentration (significant synergy with this concentration, Fig. 4). The role of surfactant mixture in producing emulsions is evident. Moreover, Fig. 8 demonstrates the emulsion indices for various GSAIL mole fractions. Again, the highest emulsification indices are corresponding to the greatest synergy mole fraction of $\alpha_1=0.2$, bringing about 78 and 74% emulsion indices after one day and after one week, respectively. These are relevant to 40.8 and 52.6% synergy (same aspect of IFT synergy). Meanwhile, monitoring after two-months, showed no significant reduction in the emulsion volumes, approving the stability. This is a consequence of surfactants regular orientation at the interface of drops, creating hydrophilic protective layers⁴⁰. Notably, achieving stable emulsions with conventional surfactants, regularly necessitates using co-surfactants that are volatile and environmentally hazardous⁷; hence, no co-surfactant was used here.

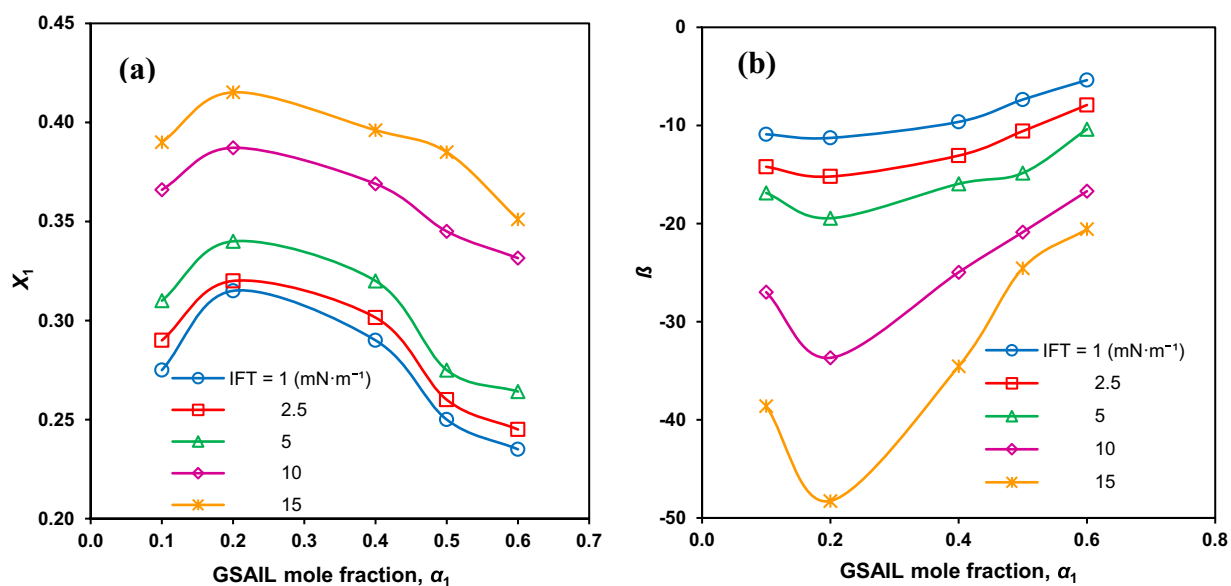


Fig. 6. Interface mole fraction (a) and interaction parameter (b) as functions of mole fraction for certain IFTs.

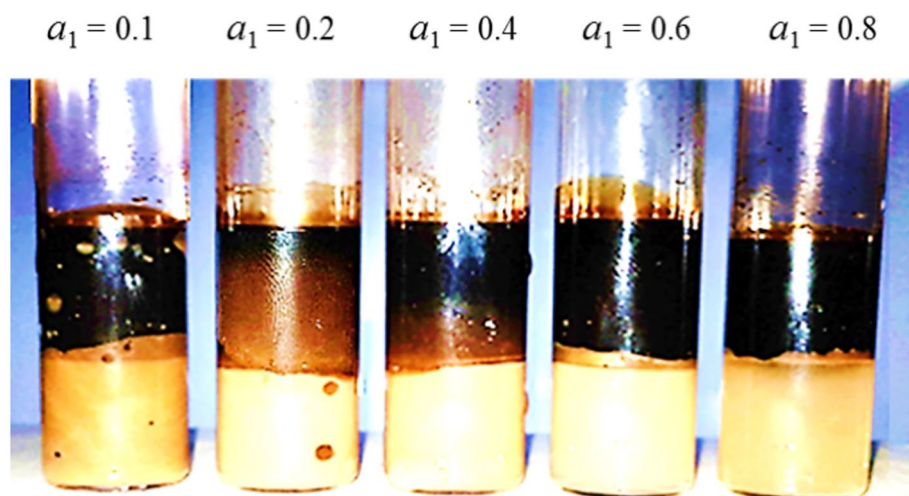


Fig. 7. The crude oil–water emulsions under different mole fractions with 0.05 mol dm^{-3} of mixtures after one day.

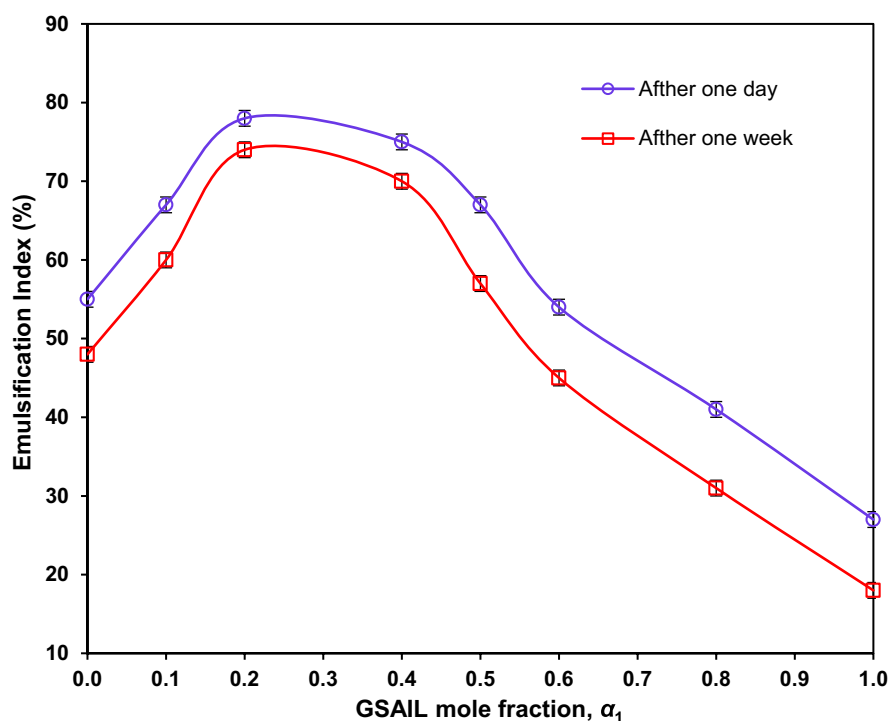


Fig. 8. The emulsification index as a function of the GSAIL mole fraction with 0.05 mol dm^{-3} of mixtures.

Wettability alteration

Wettability is crucial for reservoir rocks and their performance, affecting the residual original oil in place (OOIP). A shift of the quartz surface wettability, from oil-wet to water-wet, results in detachment of residual oil from the rocks, and improves crude oil flow. Based on CA measurements, reservoir rocks categorized as hydrophilic (water-wet, CA ranging from 0 to 80° degree), moderate (CA from 80 to 100°) and hydrophobic (oil-wet, CA from 100 to 180°)⁴¹.

In Table 5 and Fig. 9, the shapes and the corresponding wettability state, as well as measured CA of drops while surrounded are presented for different aqueous mixtures ($0.05 \text{ mol}\cdot\text{dm}^{-3}$). Notably, CAs of 130° and 70° with the GSAIL and SDBS, highly decrease to about 40° with $\alpha_1 = 0.2$. This reflects a maximum degree of synergism of 51.8%; thus, altering wettability from oil-wet to water-wet.


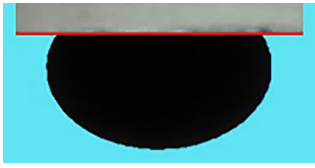
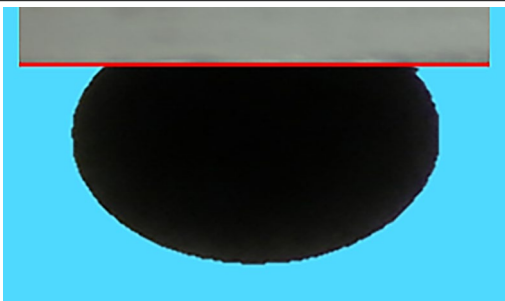
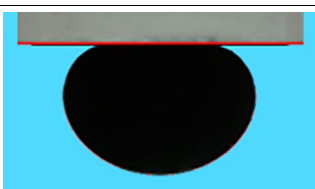
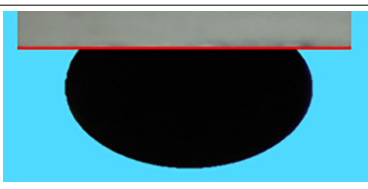
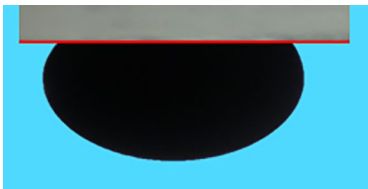
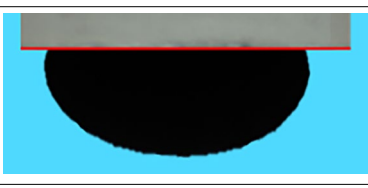
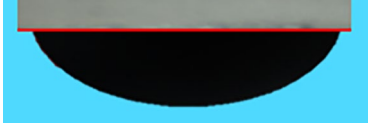

| Mole fraction | Image | Contact angle | Wettability state |
|------------------|---|---------------|-------------------|
| Pure water |  | CA = 158° | Oil-wet |
| $\alpha_1 = 0.0$ |  | CA = 70° | Water-wet |
| $\alpha_1 = 0.1$ |  | CA = 52° | Water-wet |
| $\alpha_1 = 0.2$ |  | CA = 40° | Water-wet |
| $\alpha_1 = 0.4$ |  | CA = 48° | Water-wet |
| $\alpha_1 = 0.5$ |  | CA = 60° | Water-wet |
| $\alpha_1 = 0.6$ |  | CA = 80° | Intermediate-wet |
| $\alpha_1 = 0.8$ |  | CA = 114° | Oil-wet |
| $\alpha_1 = 1.0$ |  | CA = 130° | Oil-wet |

Table 5. Shape and CA of crude oil drops on quartz surface with $0.05 \text{ mol} \cdot \text{dm}^{-3}$ of individuals and mixtures.

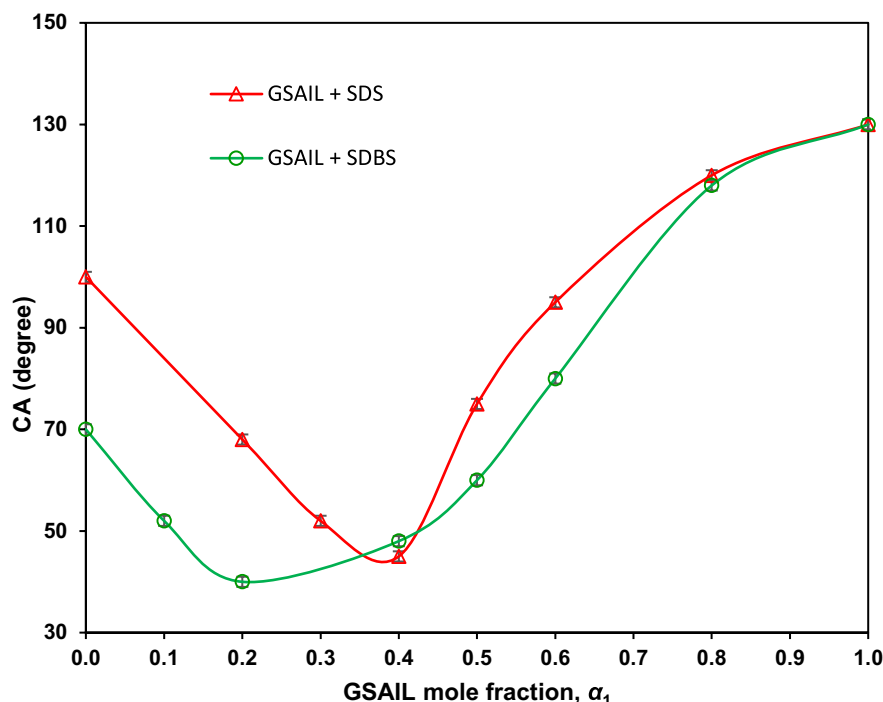


Fig. 9. Variation of CA with the GSAIL mole fraction under mixture concentration of 0.05 mol dm^{-3} .

Conclusions

This investigation was conducted to explore how effective mixtures of a nano-size imidazolium cationic GSAIL, $[\text{C}_4\text{im}-\text{C}_6\text{-imC}_4][\text{Br}_2]$, and the anionic SDBS surfactant act on the interfacial properties of the crude oil–water system. Initial results evidenced that the capability of individual surfactants was high and that IFT variations matched the Frumkin isotherm.

The adapted interactions enabled the GSAIL and SDBS surfactant to significantly reduce the IFT, surpassing the potential of a linear contribution by individual surfactants providing very distinct synergies. The mixture achieves very low IFTs at GSAIL mole fraction of only 0.2, whilst also decreasing the CMC. The variations were consistent with the NIBM model and reasonable parameter values were corresponding. Examining the emulsion formation confirmed stable crude oil in water dispersions. Consistently, wettability study showed a transition from oil-wet to water-wet due to the low adhesion of crude oil drops to the quartz surface in the present of mixtures.

Inclusively, the results affirmed that this sort of surfactant mixtures can significantly enhance the interfacial properties of the crude oil–water system. In addition to high reductions in oil–water IFT, these mixtures could alter wettability which is crucial in oil recovery. Further, the stability, confirmed through emulsion formation, gives rise feasibility of practical implications in various oilfield processes. Indeed, their effectiveness could extend to challenging conditions of high salinity and elevated temperatures which requires complementary investigations.

Data availability

The data will be provided upon request to the corresponding author of this article.

Received: 29 February 2024; Accepted: 22 August 2024

Published online: 27 August 2024

References

1. Tamayo-Mas, E., Mustapha, H. & Dimitrakopoulos, R. Testing geological heterogeneity representations for enhanced oil recovery techniques. *J. Pet. Sci. Eng.* **146**, 222–240. <https://doi.org/10.1016/j.petrol.2016.04.027> (2016).
2. Painter, P., Williams, P. & Lupinsky, A. Recovery of bitumen from Utah tar sands using ionic liquids. *Energy Fuels* **24**, 5081–5088. <https://doi.org/10.1021/ef100765u> (2010).
3. Saien, J. & Kharazi, M. The properties and applications of surface-active ionic liquids: In properties and applications of ionic liquids. *Nova Sci.* <https://doi.org/10.52305/HFEO4188> (2023).
4. Rosen, M. J. *Surfactants and Interfacial Phenomena* 3rd edn. (John Wiley and Sons, London, 2012).
5. Asadabadi, S., Saien, J. & Kharazi, M. Enhanced interfacial activity by maximizing synergy between long-chain ionic liquid and conventional surfactant for enhanced oil recovery. *RSC Adv.* **14**, 18942–18949. <https://doi.org/10.1039/D4RA02092H> (2024).
6. Gurjar, S., Sharma, S. K., Sharma, A. & Ratnani, S. Performance of imidazolium based ionic liquids as corrosion inhibitors in acidic medium: A review. *Appl. Surf. Sci. Adv.* **6**, 100170. <https://doi.org/10.1080/15422119.2022.2052094> (2021).

7. Saien, J., Kharazi, M., Pino, V. & Pacheco-Fernández, I. Trends offered by ionic liquid-based surfactants: applications in stabilization, separation processes, and within the petroleum industry. *Sep. Purif. Rev.* **52**, 164–192. <https://doi.org/10.1080/15422119.2022.2052094> (2023).
8. Jia, H. *et al.* Systematic investigation of the effects of mixed cationic/anionic surfactants on the interfacial tension of a water/model oil system and their application to enhance crude oil recovery. *Colloids Surf. A Physicochem. Eng. Asp.* **529**, 621–627. <https://doi.org/10.1016/j.colsurfa.2017.06.055> (2017).
9. Xu, Y. *et al.* Investigation on the effects of cationic surface active ionic liquid/anionic surfactant mixtures on the interfacial tension of water/crude oil system and their application in enhancing crude oil recovery. *J. Dispers. Sci. Technol.* **44**, 214–224. <https://doi.org/10.1080/01932691.2021.1942034> (2023).
10. Ezzat, A., Ayman, O., Atta, M. & Al-Lohedan, H. A. Demulsification of stable seawater/arabian heavy crude oil emulsions using star-like tricationic pyridinium ionic liquids. *Fuel* **304**, 121436. <https://doi.org/10.1016/j.fuel.2021.121436> (2021).
11. Kharazi, M. & Saien, J. Mechanism responsible altering in interfacial tension and emulsification of the crude oil-water system with nano Gemini surface active ionic liquids, salts and pH. *J. Pet. Sci. Eng.* **219**, 111090. <https://doi.org/10.1016/j.petrol.2022.111090> (2022).
12. Pillai, P., Kumar, A. & Mandal, A. Mechanistic studies of enhanced oil recovery by imidazolium-based ionic liquids as novel surfactants. *J. Ind. Eng. Chem.* **63**, 262–274. <https://doi.org/10.1016/j.jiec.2018.02.024> (2018).
13. Saien, J., Shokri, B. & Kharazi, M. Effective Synergistic action of benzimidazolium nano Gemini ionic liquid and conventional surfactant for chemical enhanced oil recovery. *ACS Omega* **9**, 22336–22344. <https://doi.org/10.1021/acsomega.4c01768> (2024).
14. Saien, J., Kharazi, M., Yarie, M. & Zolfigol, M. A. Systematic investigation of a surfactant type nano gemini ionic liquid and simultaneous abnormal salt effects on crude oil/water interfacial tension. *Ind. Eng. Chem. Res.* **58**, 3583–3594. <https://doi.org/10.1021/acs.iecr.8b05553> (2019).
15. Ding, Y. *et al.* Synthesis and demulsification performance of a Gemini ionic liquid with dual cationic active centers. *Sep. Purif. Technol.* **330**, 125242. <https://doi.org/10.1016/j.seppur.2023.125242> (2024).
16. Wang, G. *et al.* Cationic-anionic surfactant mixtures based on gemini surfactant as a candidate for enhanced oil recovery. *Colloids Surf. A: Physicochem. Eng. Asp.* **677**, 132297. <https://doi.org/10.1016/j.colsurfa.2023.132297> (2023).
17. Kharazi, M., Saien, J., Yarie, M. & Zolfigol, M. A. Promoting activity of gemini ionic liquids surfactant at the interface of crude oil-water. *Pet. Res.* **117**, 113–123. <https://doi.org/10.1021/jp9804345> (2021).
18. Kharazi, M. & Saien, J. Upgrading the properties of the crude oil–water system for eor with simultaneous effects of a homologous series of nanogemini surface-active ionic liquids, electrolytes, and pH. *ACS Omega* **7**, 40042–40053. <https://doi.org/10.1021/acsomega.2c04741> (2022).
19. Saien, J., Kharazi, M., Shokri, B., Torabi, M. & Zolfigol, M. A. A Comparative study on the design and application of new nano benzimidazolium gemini ionic liquids for curing interfacial properties of the crude oil–water system. *RSC Adv.* **13**, 15747–15761. <https://doi.org/10.1039/D3RA01783D> (2023).
20. Kharazi, M., Saien, J., Yarie, M. & Zolfigol, M. A. Different spacer homologs of Gemini imidazolium ionic liquid surfactants at the interface of crude oil-water. *J. Mol. Liq.* **296**, 111748. <https://doi.org/10.1016/j.molliq.2019.111748> (2019).
21. Kharazi, M., Saien, J., Torabi, M. & Zolfigol, M. A. Molecular design and applications of a nanostructure green tripodal surface active ionic liquid in enhanced oil recovery: Interfacial tension reduction, wettability alteration and emulsification. *Pet. Sci.* **20**, 3530–3539. <https://doi.org/10.1016/j.petsci.2023.07.010> (2023).
22. Saien, J., Shokri, B. & Kharazi, M. Synergism in mixtures of nano benzimidazolium Gemini ionic liquid and sodium dodecyl sulfate surfactants in tuning interfacial properties of crude oil–water system. *J. Mol. Liq.* **391**, 123280. <https://doi.org/10.1016/j.molliq.2023.123280> (2023).
23. Stauffer, C. E. The measurement of surface tension by the pendant drop technique. *J. Phys. Chem.* **69**, 1933–1938. <https://doi.org/10.1021/j100890a024> (1965).
24. Lan, M., Wang, X., Chen, P. & Zhao, X. Effects of surface tension and wood surface roughness on impact splash of a pure and multi-component water drop. *Case Stud. Therm. Eng.* **8**, 218–225. <https://doi.org/10.1016/j.csite.2016.07.006> (2016).
25. Taisne, L., Walstra, P. & Cabane, B. Transfer of oil between emulsion droplets. *J. Colloid Interface Sci.* **184**, 378–390. <https://doi.org/10.1006/jcis.1996.0632> (1996).
26. Kharazi, M., Saien, J., Torabi, M. & Zolfigol, M. A. Green nano multicationic ionic liquid based surfactants for enhanced oil recovery: A comparative study on design and applications. *J. Mol. Liq.* **383**, 122090. <https://doi.org/10.1016/j.molliq.2023.122090> (2023).
27. Saien, J., Eghtenaie, A. & Kharazi, M. Synergistic performance of a Gemini ionic liquid and sodium dodecyl sulfate surfactants at the crude oil-water interface. *Arab. J. Chem.* **16**, 105329. <https://doi.org/10.1016/j.arabjc.2023.105329> (2023).
28. Stubenrauch, C., Fainerman, V. B., Aksenenko, E. V. & Miller, R. Adsorption behavior and dilational rheology of the cationic alkyl trimethylammonium bromides at the water/air interface. *J. Phys. Chem. B* **109**, 1505–1509. <https://doi.org/10.1021/jp0465251> (2005).
29. Möbius, D., Miller, R. & Fainerman, V. B. *Surfactants: Chemistry, Interfacial Properties* (Elsevier, 2001).
30. Liu, G. *et al.* Thermodynamic properties of micellization of sulfo betaine-type zwitterionic gemini surfactants in aqueous solutions—A free energy perturbation study. *J. Colloid Interface Sci.* **375**, 148–153. <https://doi.org/10.1016/j.jcis.2012.02.027> (2012).
31. Zhang, L. *et al.* Ionic liquid-based ultrasound-assisted extraction of fangchinoline and tetrandrine from stephaniae tetrandrae. *J. Sep. Sci.* **32**, 3550–3554. <https://doi.org/10.1002/jssc.200900413> (2009).
32. Kumari, R., Kakati, A., Nagarajan, R. & Sangwai, J. S. Synergistic effect of mixed anionic and cationic surfactant systems on the interfacial tension of crude oil-water and enhanced oil recovery. *J. Dispers. Sci. Technol.* **40**, 1–13. <https://doi.org/10.1080/01932691.2018.1489280> (2018).
33. Kumar, H. & Kaur, G. Scrutinizing self-assembly, surface activity and aggregation behavior of mixtures of imidazolium based ionic liquids and surfactants: A comprehensive review. *Front. Chem.* **9**, 667941. <https://doi.org/10.3389/fchem.2021.667941> (2021).
34. Nabipour, M., Ayatollahi, S. & Keshavarz, P. Application of different novel and newly designed commercial ionic liquids and surfactants for more oil recovery from an iranian oil field. *J. Mol. Liq.* **230**, 579–588. <https://doi.org/10.1016/j.molliq.2017.01.062> (2017).
35. Saien, J. & Asadabadi, S. Synergistic adsorption of triton x-100 and ctab surfactants at the toluene + water interface. *Fluid Phase Equilib.* **307**, 16–23. <https://doi.org/10.1016/j.fluid.2011.04.023> (2011).
36. Olea, A. & Gamboa, C. Synergism in mixtures of cationic surfactant and anionic copolymers. *J. Colloid Interface Sci.* **257**, 321–326. [https://doi.org/10.1016/S0021-9797\(02\)00019-X](https://doi.org/10.1016/S0021-9797(02)00019-X) (2003).
37. Guang, Z. H., Caili, D. A. & Qing, Y. O. Characteristics and displacement mechanisms of the dispersed particle gel soft heterogeneous compound flooding system. *Pet. Explor. Dev.* **45**, 481–490. [https://doi.org/10.1016/S1876-3804\(18\)30053-3](https://doi.org/10.1016/S1876-3804(18)30053-3) (2018).
38. Yazhou, Z., Demin, W., Zhipeng, W. & Rui, C. The Formation and viscoelasticity of pore-throat scale emulsion in porous media. *Pet. Explor. Dev.* **44**, 111–118. [https://doi.org/10.1016/S1876-3804\(17\)30014-9](https://doi.org/10.1016/S1876-3804(17)30014-9) (2017).
39. Mandal, A., Samanta, A., Bera, A. & Ojha, K. Characterization of oil–water emulsion and its use in enhanced oil recovery. *Ind. Eng. Chem. Res.* **49**, 12756–12761. <https://doi.org/10.1021/ie101589x> (2010).
40. Gao, B. & Sharma, M. M. A family of alkyl sulfate gemini surfactants 1. characterization of surface properties. *J. Colloid Interface Sci.* **404**, 80–84. <https://doi.org/10.1016/j.jcis.2013.04.043> (2013).

41. He, L. *et al.* Interfacial sciences in unconventional petroleum production: From fundamentals to applications. *Chem. Soc. Rev.* **44**, 5446–5494. <https://doi.org/10.1039/C5CS00102A> (2015).

Acknowledgements

Financial support by the authorities of Bu-Ali Sina University is highly acknowledged.

Author contributions

J. S. did methodology, supervision, review and editing, A. E. did Experiments, conceptualization, methodology, investigation and M. K. contributed in conducting experiments, editing, software and evaluating. All authors reviewed the manuscript.

Competing interests

The authors declare no competing interests.

Additional information

Supplementary Information The online version contains supplementary material available at <https://doi.org/10.1038/s41598-024-70888-4>.

Correspondence and requests for materials should be addressed to J.S.

Reprints and permissions information is available at www.nature.com/reprints.

Publisher's note Springer Nature remains neutral with regard to jurisdictional claims in published maps and institutional affiliations.

Open Access This article is licensed under a Creative Commons Attribution-NonCommercial-NoDerivatives 4.0 International License, which permits any non-commercial use, sharing, distribution and reproduction in any medium or format, as long as you give appropriate credit to the original author(s) and the source, provide a link to the Creative Commons licence, and indicate if you modified the licensed material. You do not have permission under this licence to share adapted material derived from this article or parts of it. The images or other third party material in this article are included in the article's Creative Commons licence, unless indicated otherwise in a credit line to the material. If material is not included in the article's Creative Commons licence and your intended use is not permitted by statutory regulation or exceeds the permitted use, you will need to obtain permission directly from the copyright holder. To view a copy of this licence, visit <http://creativecommons.org/licenses/by-nc-nd/4.0/>.

© The Author(s) 2024